Journal of Breath Research

PAPER • OPEN ACCESS

Sensitive spectroscopic breath analysis by water condensation

View the article online for updates and enhancements.

Related content

Breath Biopsy Conference

BREATH BIOPSY

13th & 14th
NOVEMBER 2019
CAMBRIDGE, UK

Journal of Breath Research

PAPER

Sensitive spectroscopic breath analysis by water condensation

Kiran Sankar Maiti[1,2] (iD), Michael Lewton[2], Ernst Fill[1,2] and Alexander Apolonski[1,2,3]

1 Max-Planck-Institut für Quantenoptik, Hans-Kopfermann-Straße 1, 85748 Garching, Germany
2 Lehrstuhl für Experimental Physik, Ludwig-Maximilians-Universität München, Am Coulombwall 1, 85748 Garching, Germany
3 Novosibirsk State University, 630090 Novosibirsk, Russia

E-mail: kiran.maiti@mpq.mpg.de

Abstract

Breath analysis has great potential for becoming an important clinical diagnosis method due to its friendly and non-invasive way of sample collection. Hundreds of endogenous trace gases (volatile organic compounds (VOCs)) are present in breath, representing different metabolic processes of the body. They are not only characteristic for a person, their age, sex, habit etc, but also specific to different kinds of diseases. VOCs, related to diseases could serve as biomarkers for clinical diagnostics and disease monitoring. However, due to the large amount of water contained in breath, an identification of specific VOCs is a real challenge. In this work we present a technique of water suppression from breath samples, that enables us to identify several trace gases in breath, e.g., methane, isoprene, acetone, aldehyde, carbon monoxide, etc, using Fourier-transform infrared spectroscopy. In the current state, the technique reduces the water concentration by a factor of 2500. Sample preparation and data acquisition take about 25 min, which is clinically relevant. In this article we demonstrate the working principle of the water reduction technique. Further, with specific examples we demonstrate that water elimination from breath samples does not hamper the concentration of trace gases in breath. Preliminary experiments with real breath also indicate that the concentrations of methane, acetone and isoprene remain the same during the sample preparation.

1. Introduction

Human breath contains hundreds of volatile organic compounds (VOCs) representing different metabolic processes in the body [1, 2]. The exhaled VOCs not only provide the information about the internal chemistry of the body but also disease-specific biomarkers [3–7]. Therefore, identification of the VOCs as biomarkers is an essential task for clinical application of the breath VOCs. There are several well established techniques available for identification and quantification of VOCs. Among many, gas chromatography mass spectrometry (GC-MS), ion mobility spectrometry (IMS), proton transfer reaction mass spectrometry (PTR-MS) and selected ion flow tube mass spectrometry (SIFT-MS), electronic nose (e-nose), infrared (mid-infrared) spectroscopy, etc are most promising in breath VOCs analysis [8–15]. IMS, PTR-MS and SIFT-MS are the common soft chemical ionization techniques used for real time breath analysis, reaching sensitivities down to approximately 10 pptv. However, many small alkanes and alkenes such as ethane, whose proton affinities are less than water cannot be detected. Furthermore, the humidity in breath samples is variable and this can cause problems in interpretation owing to the dependence of product ion distributions on humidity [16]. Mid-infrared spectroscopy has no issues with detecting small alkanes and ethane. The use of the techniques of mid-infrared spectroscopy and soft chemical ionisation mass spectrometry therefore complement each other.

In general, all the existing techniques suffer from large amounts of water contained in breath and so far were facing the problem of reliable and reproducible water-free VOC detection. Water vapor contained in breath is a subject of sample collection, preparation and measurement for all the existing techniques. The dehumidification of the sample leads in all cases to improvement of the performance of the GC-MS and e-nose VOC sensors [17] and to higher detectivity in case of mid-infrared spectroscopy, as will be shown below. There are several ways to dehumidify breath samples: membranes, adsorption, digital and physical

drying. Membranes (example: Nafion tubes) do not provide sufficient water suppression [18], gas adsorption materials used for GC-MS and e-nose are still not optimal and are a subject of research in terms of extraction capacity, selectivity and reproducibility. Digital drying has been proven to be less efficient when there is real (i.e. high) water concentration in breath [19].

Here, we report on the identification and measurement of VOCs by means of dehumidified mid-infrared (with wavelength region between 3 and 20 μm) spectroscopy-based detection technique. It seems to be a possible alternative, as it has already proved the ability to identify the biological molecules in gaseous or liquid mixtures [20, 21]. The mid-infrared based techniques use the structural analysis to identify the molecules [22–26]. The mid-infrared spectral region is often called the fingerprint region because of the characteristic absorption features that can be assigned to various functional groups of molecules and vibrations. Acquisition of the spectroscopic data is fast and cost effective. The spectroscopy provides a direct way of measuring absolute VOCs concentrations by retrieving them from the amplitudes of absorption spectra. However, breath mid-infrared spectroscopy so far has not achieved the sensitivity of mass spectrometry because of two reasons: the large amount of water present in the breath and the absence of broadband powerful lasers. Recently, we reported progress in the development of a broadband high dynamic range laser mid-infrared spectrometer [27]. Up to now, 14 and 22 breath-relevant substances have been identified using different types of lasers [6, 15]. However, they were not achieved in a single, unified experiment.

Water has very broad absorption features in the mid-infrared spectral region. Unfortunately, a large part of the characteristic vibrational frequencies of VOCs occupies the same spectral region as that of water. Since most of the VOCs present in healthy human breath are at very low concentration, their absorption peaks are also very small and are easily buried under the water absorption spectra. Several attempts have been made with laser based spectroscopies in available spectral ranges, but unfortunately, due to significant water absorption spectra, identification of many molecules is not reliable [19, 28, 29]. Therefore, as a next step in this direction, one has to prepare water-free breath samples for increasing the infrared detectivity, i.e. the detection sensitivity allowing the detection of VOCs after the removal of masking factors, in our case water.
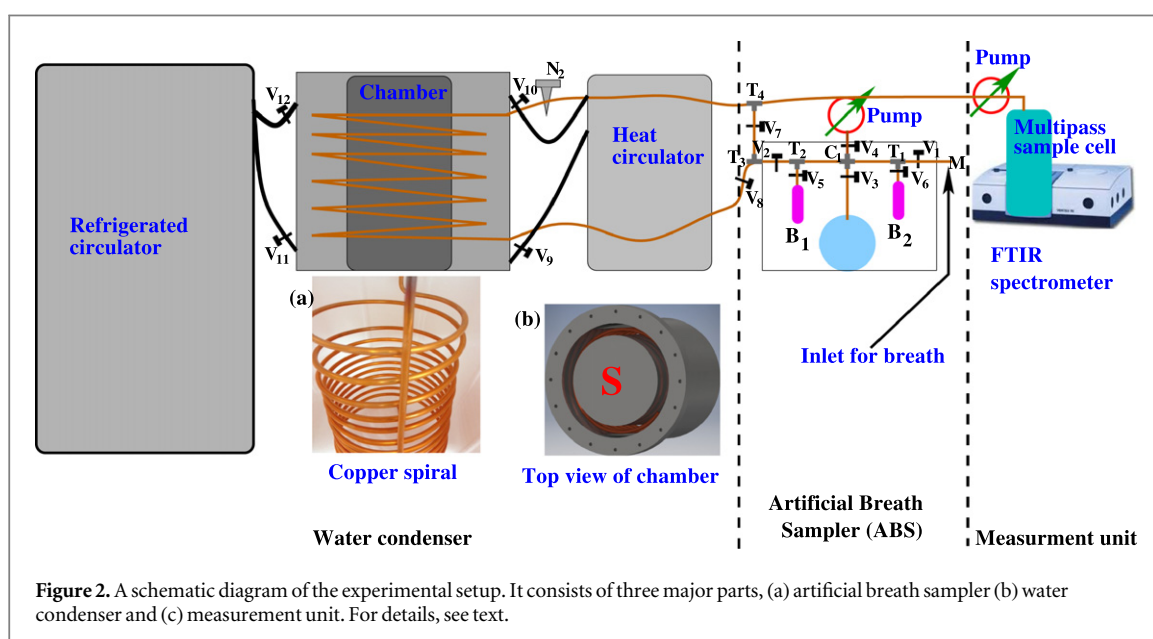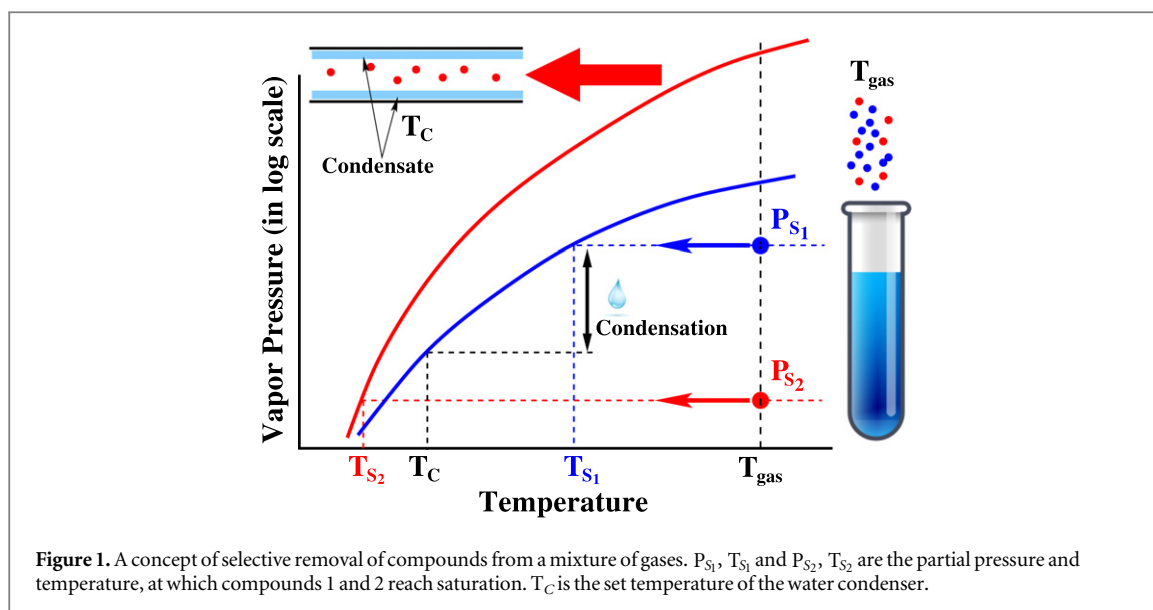
2. Method

2.1. Concept
The vapor pressure of a VOC depends upon its temperature. In equilibrium, at a fixed temperature, the number of gaseous VOCs over the liquid (or solid)

remains the same. As the temperature of the liquid is increased, the VOCs of the liquid acquire more kinetic energy, and more VOCs are released. As a result, the vapor pressure of the VOC increases. However, if the temperature of an equilibrium gaseous VOC is reduced, it loses its kinetic energy and condenses to the liquid phase. A semi-empirical correlation describing the relation between vapor pressure and its temperature for a single VOC is given by the Antone equation [30] as

$$\log_{10} P = A - \frac{B}{C + T} \qquad (1)$$

where P is the VOC vapor pressure, T is the gaseous VOC temperature and A, B and C are specific constants of the compound under study. In a gaseous VOCs mixture, if any of the compounds have lower vapor pressure than its equilibrium vapor pressure at a particular temperature, its partial pressure (and concentration) will remain the same while lowering the temperature until it reaches saturation (so-called dew point). When temperature is decreased further, the excess compounds are condensed to maintain the equilibrium vapor pressure. This situation is depicted in figure 1. Consider a mixture of two gases with concentrations S_1 and S_2 ($S_1 \gg S_2$), which are much lower than the equilibrium vapor pressure of both compounds at temperature T_{gas}. Now when the temperature of the gas VOC mixture is gradually reduced, the number of gaseous VOC remains the same until either of the compound vapors reach saturation. At temperature T_{S_1}, compound S_1 reaches its equilibrium vapor pressure and as a result, further reduction of temperature to the operating value T_c initiates its condensation and the partial pressure of S_1 compound in gas phase is reduced by the amount shown by the double arrow. On the contrary, compound S_2 at temperature T_{S_1} is still far from reaching its saturation. As a result, the partial pressure of compound S_2 in the gas phase remains the same.

This same principle is applied to breath sample preparation for mid-infrared spectroscopy. Let us consider P_{S_1} as the water partial pressure in the sample and P_{S_2} as the VOC's pressure. The operating temperature of the water condenser (see later) is T_c, where $T_{s_1} > T_c > T_{s_2}$. Therefore, when the breath sample is passed through the water condenser to the measurement cell for spectroscopic measurements, the excess amount of water vapor becomes condensed inside the water condenser. On the other hand, since $T_c > T_{s_2}$, VOCs of that type are far behind the saturation (dew point). As a result, VOCs reach the measurement cell with their original partial pressure. In real breath, water vapor is already in saturation at room temperature. Therefore, when water vapor passes through the water condenser, a large amount of its molecules become condensed there. A reduction of approximately a factor of 2500 is expected when the breath sample is passed through the cold tube at −60 °C. In addition to the condensation of compounds on the cold tube walls, their selective adhesion to the walls can occur.

Figure 1. A concept of selective removal of compounds from a mixture of gases. P_{S_1}, T_{S_1} and P_{S_2}, T_{S_2} are the partial pressure and temperature, at which compounds 1 and 2 reach saturation. T_C is the set temperature of the water condenser.

Figure 2. A schematic diagram of the experimental setup. It consists of three major parts, (a) artificial breath sampler (b) water condenser and (c) measurement unit. For details, see text.

2.2. Technical details

A schematic diagram of the experimental setup is depicted in figure 2. It consists of three major units, namely (1) artificial breath sampler (ABS), (2) water condenser and (3) sample cell and measurement unit.

(1) The artificial breath sampler is a simple arrangement which allows the mixing of different sample gases at desired proportions. It consists of a 50 cm copper tube with 3 mm inner and 6 mm outer diameter. The tube is closed at both ends with two valves (V_1 and V_2) allowing the control of the inlet and outlet of the ABS. A cross connector C_1 is attached to the middle of the tube. Both ends of the connector are closed by the valves (V_3 and V_4), followed by ISO KF-16 adaptors. One of them is connected with the vacuum Turbo pump (Oerlikon) to evacuate the ABS. To the other, a container (1 liter Restek canister) is attached, in which the mixture of gases is made. Two

T-connectors (T_1 and T_2) are attached to the copper tube equidistantly from the cross connector (C_1). A valve (V_5 or V_6) followed by a ISO KF-16 adaptor is connected to the third arm of each T-connector. This arrangement allows connecting a sample bottle (with the sample in liquid phase) by means of a flange. Two different sample bottles (B_1 and B_1) can be attached for mixing the sample gases. A T-connector T_3 is attached at the outlet of the ABS. One arm of the T-connector is directly connected to the sample cell in the spectrometer by a control valve (V_7) and the other arm is connected to the water condenser by another control valve (V_8). These two control valves allow the sample to directly pass the cell or the water condenser for water vapor suppression. All the valves, T- and cross- connectors, are from Swagelok.

(2) The water condenser is the heart of the breath sampling device that suppresses the water vapor from

a breath sample. It is a 12-meter long copper tube with the same inner and outer diameter as used for ABS, placed inside a closed cylindrical metal chamber (diameter = 20 cm and height = 20 cm) in the form of a spiral (figures 2(a) and (b)). Two ends of the copper spiral are connected to the chamber. One end of the spiral is connected with the ABS and the other end with the sample cell. The chamber has two inlets and two outlets, which are directly connected with an ultra-low refrigerated circulator (FW95-SL, Julabo Labortechnik GmbH) and a heating circulator (F32-HL). Both circulators use the same liquid as a heating or cooling medium. The operating temperature of the liquid ranges from −95 °C to +45 °C. Four valves (V_9, V_{10}, V_{11}, and V_{12}) attached with the inlets and outlets of the chamber, control the flow through the heating or cooling circulators independently. To enable fast control over temperature, the inner volume of the chamber is made as small as possible by means of a cylindrical blind spacer ((S in figure 2(b)) attached to its center.

(3) A Bruker Vertex 70 FTIR spectrometer is used to record the absorption spectra of the breath samples. The spectrometer is set to collect absorption spectra in the range between 500 cm^{-1} and 4000 cm^{-1} with a spectral resolution of 0.5 cm^{-1}. A multipass 4 m-long 'white cell' with a volume of 2 L is used to house the sample.

In the case of a liquid nitrogen cooled detector and by using the spectrometer software option for a spectral resolution of 1 cm^{-1} and 100 scans, we measured a dimensionless noise level of the device equal to 2.5×10^{-5}. Applying a signal-to-noise ratio of three, the minimum detectable concentration will be given by the equation $c_{min} = 3 \times noise/absorbance \times L$, where gas absorbance must be taken in units of ppmv-$^{-1}m^{-1}$ (see PNNL [31]) and L, the absorption path length, in m. For a typical absorption line measured in this work (acetone), with an absorbance of 5×10^{-4} and the 4 m path length of the multipass cell, this equation results in a minimum concentration of 40 ppbv.

The sample is directly transferred from the water condenser to the cell through a copper tube with the same dimension as the tube used in the water condenser and the ABS. A needle valve N_2 is connected to the water condenser in order to restrict the flow rate of sample transfer to the cell in a precisely controlled way. The spectrometer is continuously flushed with dry nitrogen to remove the water vapor and CO_2 from the spectrometer.

2.3. Samples
Chemicals to produce artificial breath are purchased from Sigma–Aldrich in liquid form. The vapor of the liquid sample is collected in ABS at room temperature. The real breath samples are collected from five healthy volunteers (no known significant health problems) aged from 35 to 77 years. The volunteers are chosen from different ethnic groups with 3:2 sex ratio. All volunteers in our research group, prior to study, signed an informed consent form. The Ludwig-Maximilians-Universität München Ethics committee has no objection to the publication of our results. Breath samples from volunteers are collected with Tedlar bags, as well as direct breathing to the ABS via mouthpiece **M** (see figure 2). In both cases one liter of breath sample is collected via normal breathing. The collection time takes less than a minute.

2.4. Operational principle
A systematic study has been carried out to optimize the water condenser and its operation. A water vapor pressure curve based on the PNNL (Pacific Northwest National Laboratory) database [31] is plotted in figure 3 as a black line. Experimental points in the optimized operating regime overlap with the PNNL line and are therefore not shown. Absorption spectra of real breath samples with reduced water vapor at three different temperatures are presented as three insets. From the spectra, efficient water suppression is evident.

The optimisation steps include adjustment of a needle valve and adjustment of a temperature of a refrigerated circulator. The needle valve connects the water condenser and a sample cell, and controls the flow of the sample. For better performance, the needle valve is located as close as possible to the chamber in order to avoid an empty space where water molecules can escape before freezing in the water condenser. Without a needle valve, the experimental water vapor pressure gradually decreases when the temperature is lowered as expected, with the slight upper shift relative to the PNNL curve (red points). The reason for that is the following: the breath sample is transferred from ABS to the sample cell under vacuum. As a result, in the beginning of the transfer, the sample passes through the water condenser very fast. Due to high speed, not all water molecules condense in the chamber and, as a result, the measured vapor pressure of water in the cell is elevated from the real vapor pressure. A systematic study indicated that 3 ml/sec is the optimum sample transfer speed for efficiently removing the water vapor.

Without a heat circulator in the water condenser, repetitive sample measurements will lead to water ice formation on the inner walls (see inset of figure 1) of the copper spiral tube shown in figure 2(a). Due to low thermal conductivity of ice, the breath sample temperature will stay higher (in case of gradual temperature lowering from room temperature) than that of the liquid and the copper spiral in the chamber. This situation is illustrated by blue points in figure 3. After switching the refrigerated circulator off, it takes hours without additional measures until the temperature of liquid in the chamber comes up to room temperature.
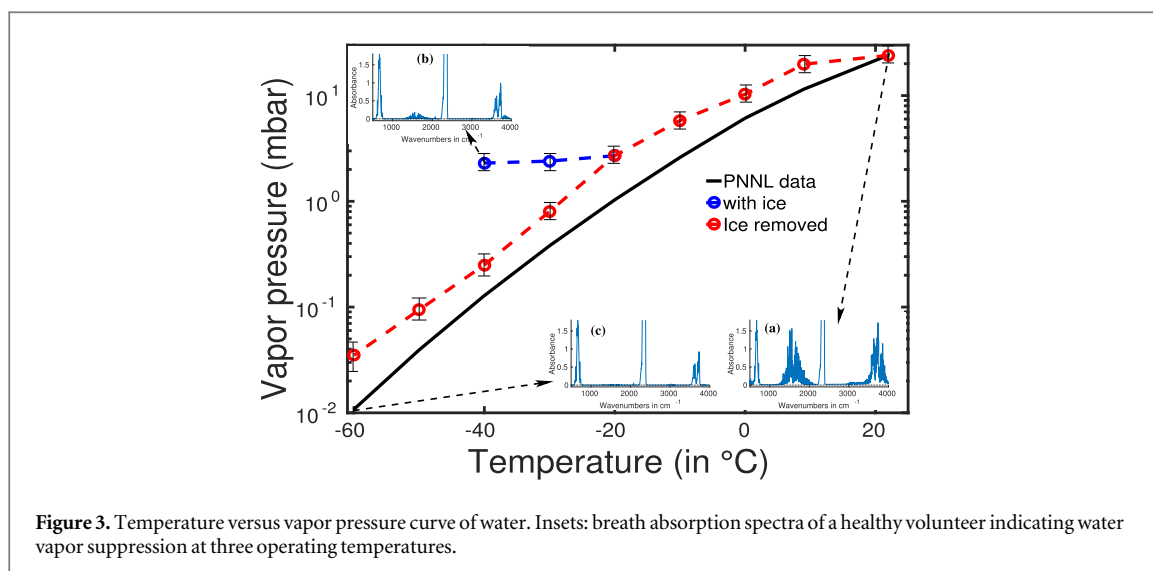
Figure 3. Temperature versus vapor pressure curve of water. Insets: breath absorption spectra of a healthy volunteer indicating water vapor suppression at three operating temperatures.

Table 1. List of molecules used for artificial breath experiment. HC stands for the hydrocarbon and VP is vapor pressure. The concentrations of substances are chosen in such a way that their dew points are far behind the operating temperature. For some substances, concentrations are chosen that are high enough so that they reach the dew point at the operation temperature.

| CAS number	Molecule	Formula	Class of Molecule	No. of Carbon atoms	Saturation at $-60\ ^{\circ}$C		Sample Used ppmv
					VP mbar	concentration ppmv	
592-76-7	1-hepten	C_7H_{14}	HC/Alkene	7	0.16	160	~45
78-79-5	isoprene	C_5H_8	Branched HC/Alkadienes	5	6.6	6600	~20
5989-27-5	limonene	$C_{10}H_{16}$	Cyclic HC/alkene	10	1.3×10^{-3}	1.3	~1
67-64-1	acetone	C_3H_6O	Ketone	3	1.3	1300	~70
591-78-6	2-hexanone	$C_6H_{12}O$	Ketone	6	7×10^{-3}	7	~10
590-86-3	isovaleraldehyde	$C_5H_{10}O$	Aldehyde	5	6.6×10^{-2}	66	~240
67-56-1	methanol	CH_3OH	Alcohol	1	—	—	~16
67-63-0	2-propanol	C_3H_8O	Alcohol	3	2.6×10^{-2}	26	~4
109-89-7	diethylamine	$C_4H_{11}N$	Amine	4	1.7	1700	~50
75-08-1	ethanethiol	C_2H_6S	Sulfur containing	2	6.2	6200	~850

With the heat circulator shown in figure 2, it takes 50 minutes to start and finish the experiment at two temperatures. After each sample preparation, the refrigerated circulator is blocked by two valves V_{11} and V_{12} attached to the corresponding inlet–outlet, and the inlet–outlet for the heat circulator is opened with valves V_9 and V_{10}. The heat circulator warms the liquid up to $+45\ ^{\circ}$C within a few minutes and the ice is melted. Finally, using a vacuum pump, the spiral is evacuated, which removes all water molecules deposited during the last sample preparation. The system is again ready for the next sample preparation.

3. Results

3.1. Vapor pressure law
To demonstrate the efficiency and potential of the water removal system in breath research, artificial breath was studied first. Artificial breath may be defined as a mixture of several gases similar to real breath. In this study, artificial breath has been prepared by mixing real breath with some VOCs at

known concentrations. The concentrations should be low enough, but higher than that present in human breath, so it can be easily detected and quantified. The selection of compounds covers most classes of molecules (e.g., hydrocarbons, alcohols, aldehydes, amines, sulfur containing molecules etc) observed in human breath. Moreover, compounds are chosen such that their boiling points are well below and above the water boiling point. The chosen molecules with the corresponding CAS numbers and classes are depicted in table 1. The results of our systematic study for nine compounds are presented in figure 4. The concentrations of limonene, 1-heptane, 2-hexanone and isovaleraldehyde are chosen in such a way that they reach the dew points within the limits of the water condenser temperature range. For example, about 45 ppmv 1-heptane has been mixed with one liter of normal breath, which corresponds to its vapor pressure of approximately 0.045 mbar. At the corresponding concentration, the substance reaches saturation at $-64\ ^{\circ}$C. As a result, when artificial breath is sent through the cold spiral in the chamber at temperatures higher than $-64\ ^{\circ}$C, only water is removed, but the
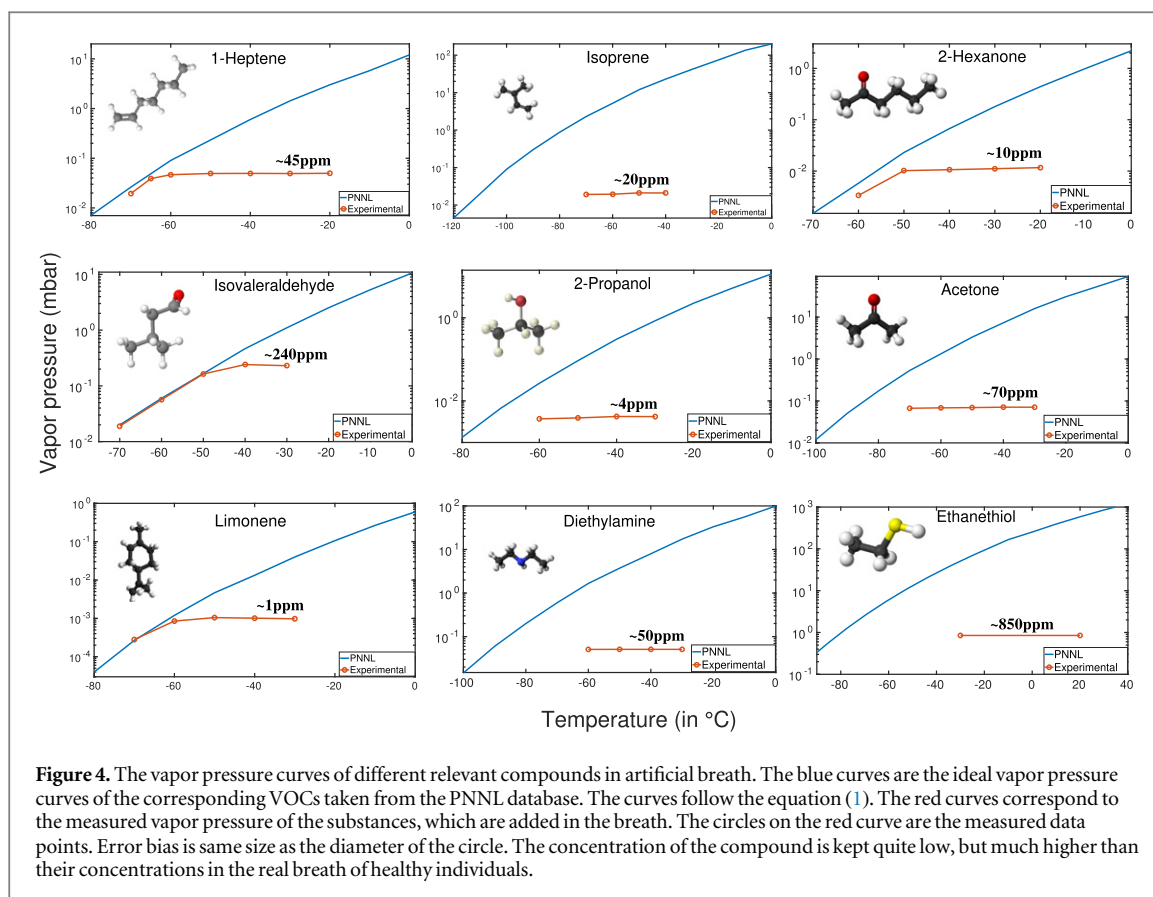
Figure 4. The vapor pressure curves of different relevant compounds in artificial breath. The blue curves are the ideal vapor pressure curves of the corresponding VOCs taken from the PNNL database. The curves follow the equation (1). The red curves correspond to the measured vapor pressure of the substances, which are added in the breath. The circles on the red curve are the measured data points. Error bias is same size as the diameter of the circle. The concentration of the compound is kept quite low, but much higher than their concentrations in the real breath of healthy individuals.

concentration of 1-heptane remains the same. Below $-64\,^{\circ}$C, the vapor pressure of 1-heptane starts decreasing by following the vapor pressure curve. In case of isoprene, the chosen concentration is only 20 ppmv, which should reach saturation at $-110\,^{\circ}$C. The measurements from $-40\,^{\circ}$C down to $-70\,^{\circ}$C yield a straight line. Among the chosen compounds, 2-hexanone has a boiling point of 128 $^{\circ}$C and a boiling point of limonene is 176 $^{\circ}$C, which are well above the boiling point of water. However, the constant vapor pressure curve above the dew point in figure 4 indicates that the condensation of the compound does not depend upon their boiling points, but rather depend only on the concentration.

It is worth noting that another mechanism of compound deposition on the inner walls of the spiral can be revealed, namely adsorption. It depends on the temperature and material of the surface. Our experiment with artificial breath demonstrates no noticeable adsorption of molecules on the copper surface because of two observations: a constant vapor pressure curve for compounds at temperatures above the dew point shown in figure 4, and lossless transfer of compounds under study from ABS to the measurement unit provided by pressure gauges at both sites.

3.2. Molecular identifications in real breath
As the second step, we identified several VOCs in the breath of healthy volunteers. All the VOCs spectra and their concentrations, presented in the following

sections, correspond to a single healthy volunteer except for carbon monoxide corresponding to five volunteers.

3.2.1. Isoprene
Isoprene is reported as being one of the main endogenous hydrocarbons in human breath [32]. It is produced as a by-product of cholesterol synthesis during the conversion of mevalonate to mevanolate-5-pyrophos-phate and isopentenyl pyrophosphate [33]. A large range of its variation (more than a factor of 50, from 20 to 1000 ppbv) is reported for different age groups of healthy volunteers in rest [34, 35]. However, the concentration of isoprene drastically varies by a factor of 3 to 4 during physical exercise [36, 37]. It is also reported that isoprene concentration varies by a similar factor during sleep [38, 39]. According to PNNL data (red curve in figure 5), isoprene yields a double spectral peak structure around 900 cm^{-1}. A similar structure of two sharp peaks was observed at 893 cm^{-1} and 906 cm^{-1} in the experiment (black line). Therefore, in our experiment it was identified as isoprene. The measured concentration of isoprene is 480 ppbv, which is in the range of the reported isoprene concentrations for healthy volunteers [34, 35]. Isoprene also exhibits other characteristic peaks at the shoulder of CO_2 peak at 992 cm^{-1} and at 1607 cm^{-1} (see figure 9). The spectral feature around 950 cm^{-1} in figure 5 is explained in section 3.2.5.
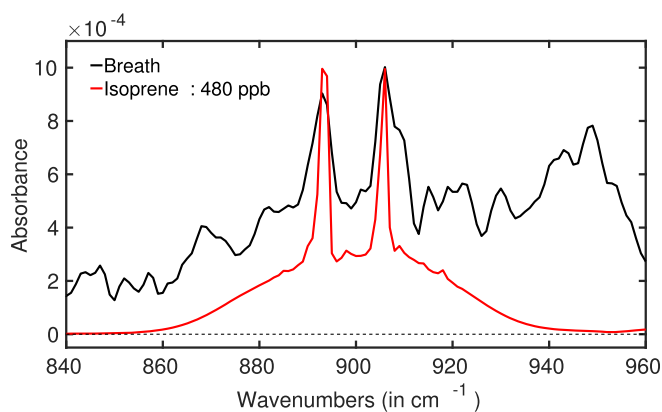
Figure 5. The spectral range where isoprene is identified from real breath. The measured concentration of isoprene is 480 ppbv for a healthy volunteer. Breath collection has been provided via direct breathing.
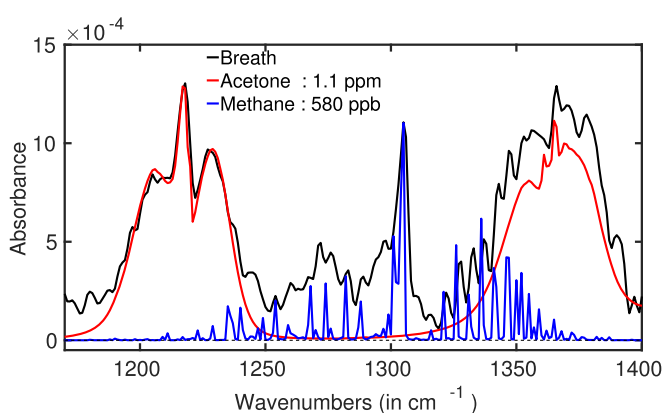
Figure 6. Acetone and methane spectra in real breath of a healthy low-methane emitter. The main source of the methane in the volunteer's breath (representing a low-methane emitter) is the inhaled ambient air. The concentration of acetone is consistent with the literature values [19, 29]. Breath collection has been provided via direct breathing.

3.2.2. Acetone

Acetone is formed from fatty acid oxidation and is present in breath as an important endogenous VOC. In general, it exhibits a low concentration in healthy individuals, however during fasting the acetone concentration increases [2]. A sweet odour characteristic for diabetic patients is well known as being due to a significant increase in the level of acetone. The geometric mean of acetone concentration in the breath of 30 healthy individuals is reported to be about 477 ppbv [40], however the absolute concentrations vary in the range of 148–2744 ppbv. It is also reported that acetone concentration varies from five up to nine times for healthy individuals depending upon the diet and the time after a meal [39, 41, 42]. Acetone is identified by two broad peaks centered at 1217 cm^{-1} and 1365 cm^{-1}. A fitting curve for acetone is plotted as a red line along with the breath spectra of a healthy volunteer in figure 6 shown as a black line. The measured concentration of acetone ~1.1 ppmv is in good agreement with the concentrations cited above. The peak centered at 1217 cm^{-1} appears with two prominent double shoulders at 1207 cm^{-1} and

1229 cm^{-1}. The broad peak centered at 1365 cm^{-1} is slightly higher in strength than that derived from the PNNL database fitting curve, indicating an overlap of characteristic aldehyde and acetone peaks (a blue curve in figure 9). The strongest acetone peak was observed at 1750 cm^{-1} (not shown).

3.2.3. Methane

Methane is an endogenous VOC, which traditionally divides the whole population into two parts; 'methane emitters' and 'methane non-emitters'. It is reported that approximately 50% of the population are methane emitters [2], this strongly depends on ethnic origin, diet, bacterial flora, and intestinal transit time [43]. However, recent publications show that such a division is not fully correct [44]. Three groups were identified: low, moderate and high methane emitters. The concentration of methane in breath strongly varies over time [39, 45]. In general, methane is produced by methanogens in the large intestine. Specific methane spectral features are identified in a healthy moderate methane emitter breath around 3000 cm^{-1} (see figure 7). The P, Q and R branches of
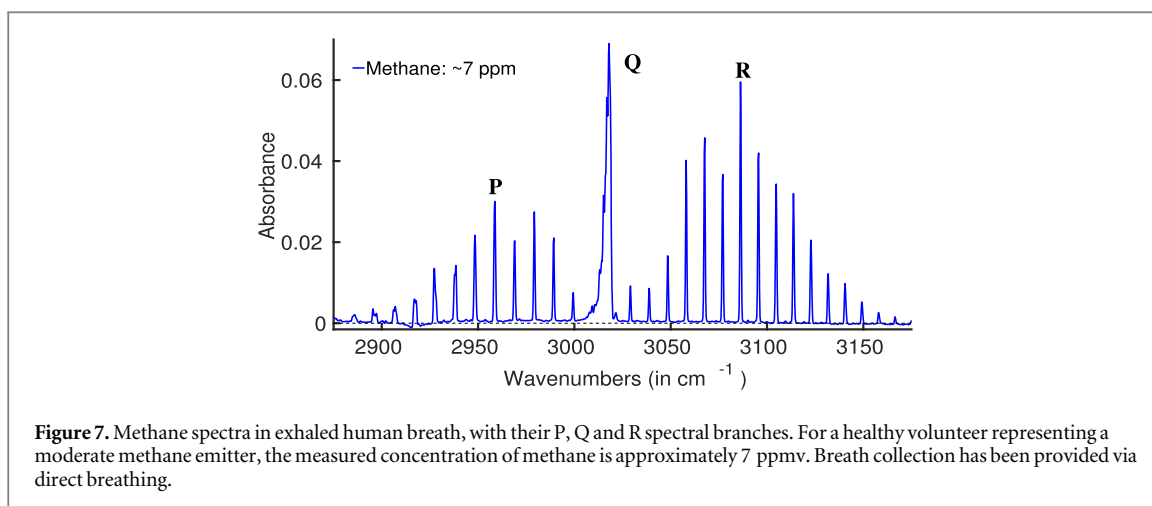
Figure 7. Methane spectra in exhaled human breath, with their P, Q and R spectral branches. For a healthy volunteer representing a moderate methane emitter, the measured concentration of methane is approximately 7 ppmv. Breath collection has been provided via direct breathing.
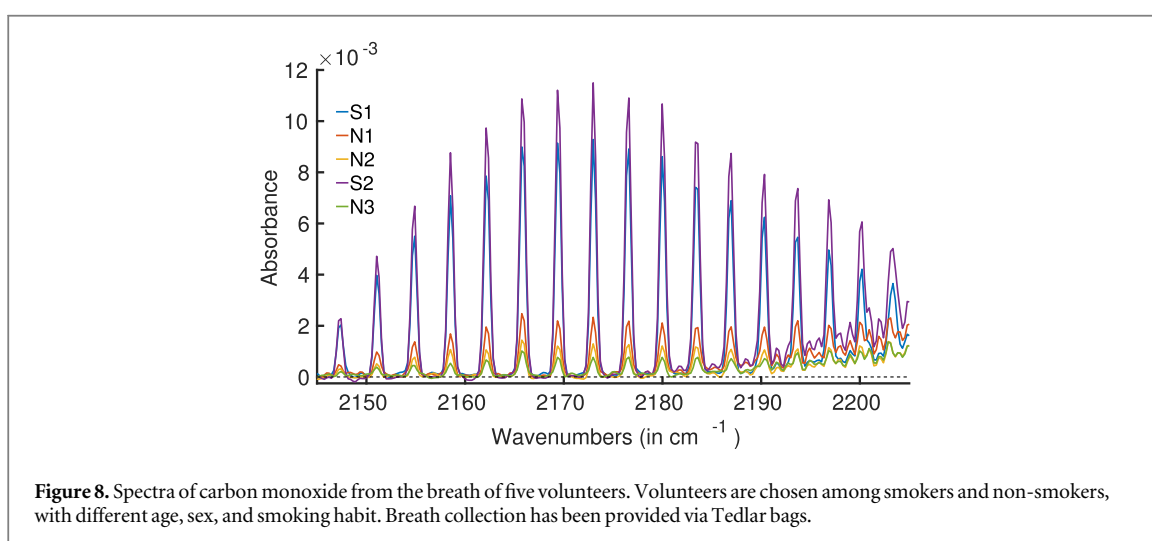
Figure 8. Spectra of carbon monoxide from the breath of five volunteers. Volunteers are chosen among smokers and non-smokers, with different age, sex, and smoking habit. Breath collection has been provided via Tedlar bags.

methane are observed at around $2960 \, cm^{-1}$, $3018 \, cm^{-1}$ and $3086 \, cm^{-1}$ respectively. Methane is also identified in another region, with its P, Q, R branches located at $1274 \, cm^{-1}$, $1305 \, cm^{-1}$ and $1336 \, cm^{-1}$ respectively (see figure 6).

3.2.4. Carbon monoxide
The main source of carbon monoxide (CO) in human breath is smoking, either active or passive. After smoke is inhaled, CO enters the blood from the alveolar membrane and bonds with the haemoglobin to produce the semi-stable compound carboxyhaemoglobin. CO is released back from the alveolae up to several hours after inhalation [46]. In addition to external sources, CO is also produced by oxidative stress in the lung and inflammatory tissue injury [47]. In the experiment, the characteristic CO spectrum is observed around $2170 \, cm^{-1}$. In mid-infrared spectra of human breath, it is not generally visible because of its coincidence with water absorption. In our experiment, effective water suppression makes the CO visible. The corresponding CO spectra are presented in figure 8, where 'S' indicates a smoker and 'N' a non-smoker. Interestingly, there is a large variation of CO concentration in breath for smokers and non-

smokers. For non-smoker's, the measured concentration of CO is about 1 ppmv. Among smokers, the CO concentration depends on the number of cigarettes smoked during a day and the interval between the last cigarette and the measurement.

3.2.5. Aldehyde and carbon dioxide
Several aldehydes are found as VOCs in breath, among them are formaldehyde, acetaldehyde, hexanal and heptanal [48, 49]. In mid-infrared spectra, all aldehydes, according to PNNL data, exhibit a strong absorption peak around $1750 \, cm^{-1}$. As we already identified in the acetone section, a comparable acetone characteristic peak was also observed at the same spectral position, with a similar spectral strength. In the breath spectra of a healthy individual a strong, rather broad absorption peak was observed at $1750 \, cm^{-1}$, of almost double in strength in comparison to the recorded acetone signal (see figure 9). Therefore, this broad peak was attributed to a mixture of comparable characteristic aldehyde and acetone peaks. Another broad but relatively small absorption peak should appear around $1365 \, cm^{-1}$. Because of the strong acetone peak at the same wavenumber position, this peak is also difficult to identify separately.
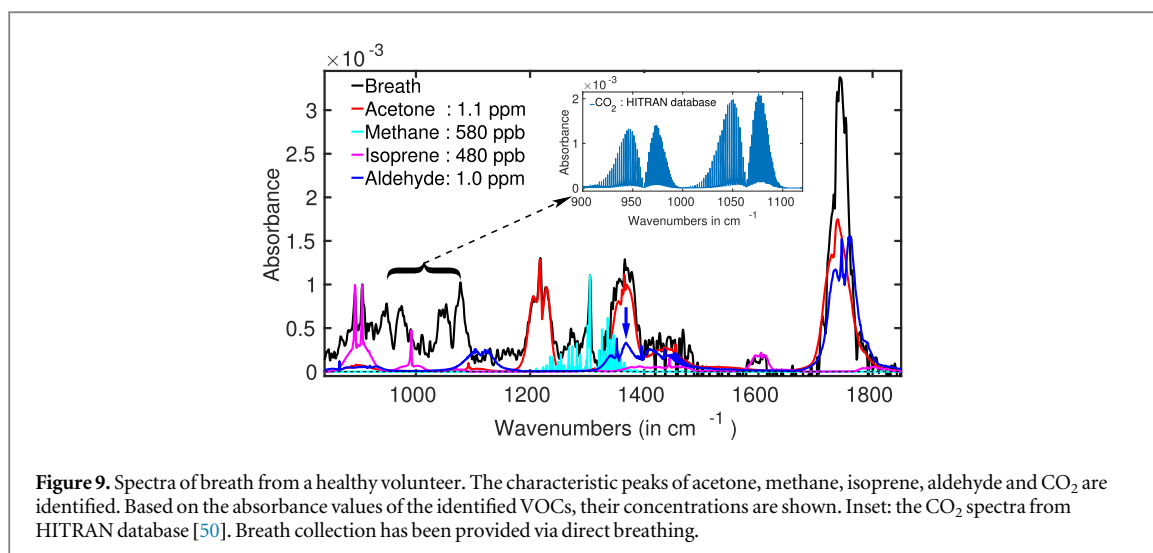
Figure 9. Spectra of breath from a healthy volunteer. The characteristic peaks of acetone, methane, isoprene, aldehyde and CO_2 are identified. Based on the absorbance values of the identified VOCs, their concentrations are shown. Inset: the CO_2 spectra from HITRAN database [50]. Breath collection has been provided via direct breathing.

Nevertheless, the overlap of the two elevates the peak of acetone at 1365 cm^{-1} (see the arrow in figure 9). The measured concentration of all aldehydes present in the breath is 1.0 ppmv, which is in agreement with literature [4].

Two double spectral features are observed in mid-infrared breath spectra at 946 cm^{-1}, 975 cm^{-1} and 1050 cm^{-1}, 1076 cm^{-1}. These four peaks are identified as CO_2 spectral features. The inset in figure 9 shows the corresponding CO_2 spectral features plotted from the HITRAN database. Due to the very strong absorption peak of CO_2 at 2300 cm^{-1} in breath, these low intensity peaks have so far not been discussed in the breath literature. In fact, these peaks are clearly visible only after water removal from the breath sample. Here we note that these CO_2 peaks may cause misinterpretation of other compounds having absorption bands in this spectral region.

4. Conclusions

A water-eliminated breath sample preparation technique has been developed for mid-infrared spectroscopy. The operational principle with necessary technical details is presented together with its verification by means of artificial breath. Water reduction by a factor of approximately 2500 has been achieved at an operating temperature of $-60\,^{\circ}$C. We show that the water reduction procedure we used does not reduce concentrations of VOCs present in breath at low concentrations. The current setup has the capability for water reduction by another factor of 100 by further lowering the operating temperature down to $-90\,^{\circ}$C. The technique can be used by GC-MS and e-nose VOC detections.

FTIR spectroscopy has been used to record the absorption spectra of water-eliminated breath samples. Due to the water removal, several VOCs have become visible with their characteristic spectral features. The amplitude of the corresponding absorption peak allows one to quantify an absolute concentration of the VOC in the breath sample. Specifically, it was done by measuring VOC's absorption amplitude and comparing it with the PNNL data. Acetone, methane, isoprene, aldehyde, carbon monoxide and carbon dioxide have been identified. The corresponding spectrum landscape provides reliable information about relative and absolute concentrations for most of the VOCs. We are not aware of the published results identifying isoprene in breath by mid-infrared spectroscopy. Observing the carbon monoxide levels in exhaled breath, smokers and non-smokers have been unambiguously distinguished. With the present experimental setup, a detectivity of 50 ppbv is reached. Further improvement of this parameter using both laser based technology and further water suppression is expected to reach the pptv level of VOCs concentrations, comparable with the level of GC-MS .

Acknowledgments

ORCID iDs

Kiran Sankar Maiti https://orcid.org/0000-0002-7337-7541

References

[1] Pauling L, Robinson A B, Teranishi R and Cary P 1971 Quantitative analysis of urine vapor and breath by gas-liquid partition chromatography *Proc. Natl. Acad. Sci.* **68** 2374–6

[2] de L, Costello B, Al-Kateb H, Flynn C, Filipiak W, Khalid T, Osborne D and Ratcliffe N M 2014 A review of the volatiles from the healthy human body *J. Breath Res.* **8** 014001

[3] Phillips M, Cataneo R N, Ditkoff B A, Fisher P, Greenberg J, Gunawardena R, Kwon C S, Rahbari-Oskoui F and Wong C 2003 Volatile markers of breast cancer in the breath *The Breast Journal* **9** 184–91

[4] Fuchs P, Loeseken C, Schubert J K and Miekisch W 2010 Breath gas aldehydes as biomarkers of lung cancer *Int. J. Cancer* **126** 2663–70

[5] Prabhakar A, Quach A, Zhang H, Terrera M, Jackemeyer D, Xian X, Tsow F, Tao N and Forzani E S 2015 Acetone as biomarker for ketosis buildup capability—a study in healthy individuals under combined high fat and starvation diets *Nutr. J.* **14** 41

[6] Wang C and Sahay P 2009 Breath analysis using laser spectroscopic techniques: Breath biomarkers, spectral fingerprints, and detection limits *Sensors* **9** 8230–62

[7] Amann A and Smith D (ed) 2013 *Volatile Biomarkers: Non-Invasive Diagnosis in Physiology and Medicine* (Amsterdam: Elsevier)

[8] Phillips M, Herrera J, Krishnan S, Zain M, Greenberg J and Cataneo R N 1999 Variation in volatile organic compounds in the breath of normal humans *J. Chromatogr. B: Biomed. Sci. Appl.* **729** 75–88

[9] Ruzsanyi V, Fischer L, Herbig J, Ager C and Amann A 2013 Multi-capillary-column proton-transfer-reaction time-of-flight mass spectrometry *J. Chromatogr. A* **1316** 112–8

[10] Natale C D, Paolesse R, Martinelli E and Capuano R 2014 Solid-state gas sensors for breath analysis: a review *Anal. Chim. Acta* **824** 1–17

[11] Lanucara F, Holman S W, Gray C J and Eyers C E 2014 The power of ion mobility-mass spectrometry for structural characterization and the study of conformational dynamics *Nat. Chem.* **6** 281–94

[12] Lamote K, Brinkman P, Vandermeersch L, Vynck M, Sterk P J, Langenhove H V, Thas O, Cleemput J V, Nackaerts K and van Meerbeeck J P 2017 Breath analysis by gas chromatography-mass spectrometry and electronic nose to screen for pleural mesothelioma: a cross-sectional case-control study *Oncotarget* **8** 91593–602

[13] Nakhleh M K *et al* 2017 Diagnosis and classification of 17 diseases from 1404 subjects via pattern analysis of exhaled molecules *ACS Nano* **11** 112–25 PMID: 28000444

[14] Blake R S, Monks P S and Ellis A M 2009 Proton-transfer reaction mass spectrometry *Chem. Rev.* **109** 861–96 pMID: 19215144

[15] Muraviev A V, Smolski V O, Loparo Z E and Vodopyanov K L 2018 Massively parallel sensing of trace molecules and their isotopologues with broadband subharmonic mid-infrared frequency combs *Nat. Photon.* **12** 209–14

[16] Ellis A M and Mayhew C A 2014 *Proton Transfer Reaction Mass Spectrometry: Principles and Applications* (New York: Wiley)

[17] Haick H, Broza Y Y, Mochalski P, Ruzsanyi V and Amann A 2014 Assessment, origin, and implementation of breath volatile cancer markers *Chem. Soc. Rev.* **43** 1423–49

[18] Nafion chemical retention/losses and selectivity http://permapure.com/products/nafion-tubing/nafion-dryer-performance-and-selectivity/ accessed: 2018

[19] Reyes-Reyes A, Hou Z, van Mastrigt E, Horsten R C, de Jongste J C, Pijnenburg M W, Urbach H P and Bhattacharya N 2014 Multicomponent gas analysis using broadband quantum cascade laser spectroscopy *Opt. Express* **22** 18299–309

[20] Perez-Guaita D, Garrigues S and de la Guardia M 2014 Infrared-based quantification of clinical parameters *TRAC Trends Anal. Chem.* **62** 93–105

[21] Baker M J *et al* 2014 Using fourier transform ir spectroscopy to analyze biological materials *Nat. Protocols* **9** 1771–91

[22] Maiti K S, Samsonyuk A, Scheurer C and Steinel T 2012 Hydrogen bonding characteristics of 2-pyrrolidinone: a joint experimental and theoretical study *Phys. Chem. Chem. Phys.* **14** 16294–300

[23] Maiti K S 2015 Vibrational spectroscopy of methyl benzoate *Phys. Chem. Chem. Phys.* **17** 19735–44

[24] Maiti K S 2015 Broadband two dimensional infrared spectroscopy of cyclic amide 2-pyrrolidinone *Phys. Chem. Chem. Phys.* **17** 24998–5003

[25] Peuker S, Andersson H, Gustavsson E, Maiti K S, Kania R, Karim A, Niebling S, Pedersen A, Erdelyi M and Westenhoff S 2016 Efficient isotope editing of proteins for site-directed vibrational spectroscopy *J. Am. Chem. Soc.* **138** 2312–8 pMID: 26796542

[26] Roy S and Maiti K S 2018 Structural sensitivity of CH vibrational band in methyl benzoate *Spectrochim. Acta Mol. Biomol. Spectrosc.* **196** 289–94

[27] Pupeza I *et al* 2015 High-power sub-two-cycle mid-infrared pulses at 100 MHz repetition rate *Nat. Photon.* **9** 721

[28] Kamat P C, Roller C B, Namjou K, Jeffers J D, Faramarzalian A, Salas R and McCann P J 2007 Measurement of acetaldehyde in exhaled breath using a laser absorption spectrometer *Appl. Opt.* **46** 3969–75

[29] Reyes-Reyes A, Horsten R C, Urbach H P and Bhattacharya N 2015 Study of the exhaled acetone in type 1 diabetes using quantum cascade laser spectroscopy *Anal. Chem.* **87** 507–12 PMID: 25506743

[30] Reid R C, Prausnitz J M and Sherwood T K 1977 *Properties of Gases and Liquids* (New York: McGraw-Hill)

[31] Johnson T J, Sams R L and Sharpe S W 2004 The PNNL quantitative infrared database for gas-phase sensing: a spectral library for environmental, hazmat, and public safety standoff detection *Proc. SPIE 5269 Chemical and Biological Point Sensors for Homeland Defense* vol 5269 159–67

[32] Gelmont D, Stein R A and Mead J F 1981 Isoprene the main hydrocarbon in human breath *Biochem. Biophys. Res. Commun.* **99** 1456–60

[33] Sharkey T D 1996 Isoprene synthesis by plants and animals *Endeavour* **20** 74–8

[34] Taucher J, Hansel A, Jordan A, Fall R, Futrell J H and Lindinger W 1997 Detection of isoprene in expired air from human subjects using proton transfer reaction mass spectrometry *Rapid Commun. Mass Spectrom.* **11** 1230–4

[35] Karl T, Prazeller P, Mayr D, Jordan A, Rieder J, Fall R and Lindinger W 2001 Human breath isoprene and its relation to blood cholesterol levels: new measurements and modeling *J. Appl. Physiol.* **91** 762–70 PMID: 11457792

[36] King J, Kupferthaler A, Unterkofler K, Koc H, Teschl S, Teschl G, Miekisch W, Schubert J, Hinterhuber H and Amann A 2009 Isoprene and acetone concentration profiles during exercise on an ergometer *J. Breath Res.* **3** 027006

[37] King J, Koc H, Unterkofler K, Mochalski P, Kupferthaler A, Teschl G, Teschl S, Hinterhuber H and Amann A 2010 Physiological modeling of isoprene dynamics in exhaled breath *J. Theor. Biol.* **267** 626–37

[38] Cailleux A and Allain P 1989 Isoprene and sleep *Life Sciences* **44** 1877–80

[39] Maiti K S, Lewton M, Fill E and Apolonski A 2018 Breath analysis: from an individual's island of stability to comparison of cohorts *Sci. Rep.* Submitted

[40] Turner C, Španěl P and Smith D 2006 A longitudinal study of ammonia, acetone and propanol in the exhaled breath of 30 subjects using selected ion flow tube mass spectrometry, sift-ms *Physiol. Meas.* **27** 321

[41] Španěl P, Dryahina K, Rejšková A, Chippendale T W E and Smith D 2011 Breath acetone concentration; biological variability and the influence of diet *Physiol. Meas.* **32** N23

[42] Anderson J C 2015 Measuring breath acetone for monitoring fat loss: Review *Obesity (Silver Spring, Md.)* **23** 2327–34

[43] Florin T H J, Zhu G, Kirk K M and Martin N G 2000 Shared and unique environmental factors determine the ecology of methanogens in humans and rats *Am. J. Gastroenterol.* **95** 2872–9

[44] Dryahina K, Smith D and Španěl P 2010 Quantification of methane in humid air and exhaled breath using selected ion flow tube mass spectrometry *Rapid Commun. Mass Spectrom.* **24** 1296–304

[45] Polag D and Keppler F 2018 Long-term monitoring of breath methane *Sci. Total Environ.* **624** 69–77

[46] Ryter S W and Sethi J M 2007 Exhaled carbon monoxide as a biomarker of inflammatory lung disease *J. Breath Res.* **1** 026004

[47] Ryter S W 2010 Special issue on carbon monoxide and exhaled biomarkers in human disease *J. Breath Res.* **4** 040201

[48] Turner C, Španěl P and Smith D 2006 A longitudinal study of ethanol and acetaldehyde in the exhaled breath of healthy volunteers using selected-ion flow-tube mass spectrometry *Rapid Commun. Mass Spectrom.* **20** 61–8

[49] Schwarz K, Filipiak W and Amann A 2009 Determining concentration patterns of volatile compounds in exhaled breath by ptr-ms *J. Breath Res.* **3** 027002

[50] Gordon I E *et al* 2017 The hitran2016 molecular spectroscopic database *J. Quant. Spectrosc. Radiat. Transfer* **203** 3–69